Human Molecular Genetics, 2017, Vol. 26, No. 19 3653–3662

doi: 10.1093/hmg/ddx223
Advance Access Publication Date: 15 June 2017
Original Article

ORIGINAL ARTICLE

Overexpression of microRNAs from the *Gtl2-Rian* locus contributes to postnatal death in mice

Soichiro Kumamoto[1], Nozomi Takahashi[1,†], Kayo Nomura[1], Makoto Fujiwara[1], Megumi Kijioka[1], Yoshinobu Uno[2], Yoichi Matsuda[2], Yusuke Sotomaru[3] and Tomohiro Kono[1,*]

[1]Department of BioScience, Tokyo University of Agriculture, Sakuragaoka, Setagaya-ku, Tokyo, Japan, [2]Graduate School of Bioagricultural Sciences, Nagoya University, Furo-cho, Chikusa-ku, Nagoya, Japan and [3]Natural Science Center for Basic Research and Development, Hiroshima University, Kasumi, Minami-ku, Hiroshima, Japan

*To whom correspondence should be addressed at: Department of BioScience, Tokyo University of Agriculture, 1-1-1 Sakuragaoka, Setagaya-ku, Tokyo 156-8502, Japan. Tel: +81 354772543; Fax: +81 354772543; Email: tomohiro@nodai.ac.jp

Abstract

The *Dlk1-Dio3* imprinted domain functions in embryonic development but the roles of noncoding RNAs expressed from this domain remain unclear. We addressed this question by generating transgenic (TG) mice harbouring a BAC carrying IG-DMR (intergenic-differentially methylated region), *Gtl2*-DMR, *Gtl2*, *Rtl1/Rtl1as*, and part of *Rian*. High postnatal lethality (>85%) of the BAC-TG pups was observed in the maternally transmitted individuals (MAT-TG), but not following paternal transmission (PAT-TG). The DNA methylation status of IG-DMR and *Gtl2*-DMR in the BAC-allele was paternally imprinted similar to the genomic allele. The mRNA-Seq and miRNA-Seq analysis revealed marked expression changes in the MAT-TG, with 1,500 upregulated and 2,131 downregulated genes. The long noncoding RNAs and 12 miRNAs containing the BAC locus were markedly enhanced in the MAT-TG. We identified the 24 target genes of the overexpressed miRNAs and confirmed the downregulation in the MAT-TG. Notably, overexpression of mir770, mir493, and mir665 from *Gtl2* in the MAT-TG embryos led to decreased expression of the 3 target genes, *Col5a1*, *Pcgf2*, and *Clip2*. Our results suggest that decreased expression of the 3 target genes concomitant with overexpression of the miRNAs within *Gtl2* may be involved in the postnatal death in the MAT-TG. Because this imprinted domain is well conserved between mice and humans, the results of genetic and molecular analysis in mice hold important implications for related human disorders such as Temple syndrome.

Introduction

The genes that are classified as imprinted genes in mammals exhibit a unique, parental-origin-specific expression pattern. Imprinted genes play a crucial role in embryonic and extra-embryonic differentiation and development (1–3), as well as in a variety of diseases after birth, a process governed by complex epigenetic mechanisms (4). The *Dlk1-Dio3* imprinted region contains the coding paternally expressed genes, *Dlk1* (mouse delta-like homolog 1), *Rtl1* (retrotransposon-like 1) and *Dio3* (type III

†Present address: Department of Genetics, University of Cambridge, Downing Street, Cambridge CB2 3EH, UK.
Received: April 5, 2017. **Revised:** May 23, 2017. **Accepted:** June 1, 2017

iodothyronine deiodinase) as well as the noncoding maternally expressed genes *Gtl2 (Meg3*, maternally expressed 3), *Rtl1as* (retrotransposon-like 1 antisense), *Rian* (RNA imprinted and accumulated in nucleus) and *Mirg* (microRNA (miRNA) containing gene) (5–9). Notably, several microRNAs (miRNAs) and small nucleolar RNAs (snoRNAs) are also derived from the maternally expressed noncoding RNAs, *Rtl1as*, *Rian*, and *Mirg*. The expression of this imprinted gene cluster is controlled by three differentially methylated regions (DMRs): the intergenic DMR (IG-DMR), *Gtl2*-DMR, and *Dlk1*-DMR (10,11). Of these, IG-DMR, which is methylated solely in the paternal allele and located at downstream of *Dlk1*, is recognised as a major regulatory element.

The 1-Mb *Dlk1-Dio3* is located on mouse distal chromosome 12 and human chromosome 14q32.2. Both maternal and paternal uniparental disomy 12 mice are embryonic lethal because of dysregulation of maternally and paternally expressed imprinted genes in the domain. In humans, uniparental disomy of maternal chromosome 14 results in Temple syndrome, which presents symptoms such as low birth weight, mytonic depression, and precocious puberty (12,13), whereas paternal uniparental disomy 14 leads to Kagami-Ogata syndrome, which shows a unique phenotype characterized by a bell-shaped small rib cage and abdominal-wall abnormalities. The imprinted domain is well conserved between mice and humans; therefore, the results of genetic and molecular analysis in mice hold important implications for the related human disorders.

Gene-deletion studies in mice have demonstrated absence of expression of imprinted gene in the *Dlk1-Dio3* domain causes pre- and postnatal developmental defects. Paternal deletion of either *Dlk1* or *Rtl1* results in several developmental disorders, such as obesity, blepharophimosis, skeletal dysplasia, elevation of serum lipid metabolites, and placental hypoplasia, and a considerably high rate of lethality is observed in both cases (14,15). Notably, *Rtl1* expression level is controlled by an RNAi mechanism mediated by *Rtl1as*, which encodes at least 7 miRNA (16). *Dio3* is known to be involved in the regulation of thyroid hormone levels in serum (17). Moreover, *Gtl2* was found to result in a developmental disorder featuring a unique inheritance mode. Specifically, when the deletion was inherited from the mother, the pups exhibited a normal phenotype at birth, but they all died within 4 weeks after birth, probably due to severely hypoplastic pulmonary alveoli and hepatocellular necrosis. Conversely, paternal deletion resulted in postnatal lethality in 75% of the pups and severe growth retardation in the survivors. More importantly, the homozygous mutants were normally born and developed into fertile adults. Thus, *Gtl2* itself is not the causative gene for the observed abnormalities (18).

It is known that some imprinted genes are dosage sensitive and therefore two-fold increase in expression resulting from biallelic expression is likely to disturb normal development. For instance, a double dose of *Dlk1* causes enhanced embryonic growth and partial postnatal lethality (19). In this study, to ask whether overdose of maternally expressed noncoding RNAs affects normal development, we generated TG mice harbouring a 147-kb bacterial artificial chromosome (BAC) clone (Vector pBACe3.6, C3H genomic library) carrying IG-DMR, *Gtl2*-DMR, *Gtl2*, *Rtl1as*/*Rtl1*, and part of *Rian*. The BAC fragment encodes 19 miRNAs, of which 9, 6 and 4 are expressed from *Gtl2*, *Rtl1as* and *Rian*, respectively. We found that 85% of the MAT-TG embryos (maternally transmitted BAC) exhibited postnatal lethality in a breeding test whereas no phenotypic disorder was detected in the PAT-TG embryos (paternally transmitted BAC). By using the bisulphite-sequencing method, we examined the methylation state of the inducing BAC allele and we performed global transcriptome analysis of mRNAs and miRNAs. Our results showed that the BAC contains a unit necessary for establishing a parental-allele-specific methylation imprint. The results also suggest that overexpression of the noncoding miRNAs, especially miRNAs, from the maternally transmitted BAC sequence are involved in postnatal lethality.

Results

Mode of phenotypic inheritance

To enhance our understanding of the functional effects of noncoding RNAs expressed from the *Gtl2-Rian* imprinted region on parental-origin-dependent phenotype, we generated BAC-TG mice harbouring a 147 kb DNA fragment extending from IG-DMR to the first half of *Rian*, which was derived from a C3H strain mouse (Fig. 1). Southern hybridisation and fluorescence *in situ* hybridization (FISH) analyses revealed that the mutant mice were harbored 3 copies of the BAC-clones, which were inserted in tandem at the 2E1 region of chromosome 2 (Supplementary Material, Fig. S1A and B).

Notably, in mating tests the BAC-TG mice exhibited parental-origin-dependent developmental phenotypes (Fig. 2). The heterozygous mutant mice that inherited the BAC-clone from the mother (MAT-TG mutants) were born in the expected Mendelian ratio (number of mice, mutant: WT = 48:42). However, the mutant pups were significantly lighter than their WT littermates (1.11 vs 1.31 g, $P < 0.01$) and 87.5% of them died within 1 week, although they presented no morphological abnormality. The survivors grew to adulthood and exhibited regular reproductive capability. In contrast, the mutants that inherited the BAC-clone from the father (PAT-TG mutants, $n = 38$) showed no abnormality at birth and grew similarly as their WT littermates ($n = 36$). Thus, the mutants exhibited parental-origin-dependent developmental phenotypes, which suggest that the BAC-clone allele in the mutants is imprinted similarly as in WT. Histological analyses showed alveolar, hepatic lobule and spleen white-pulp hypoplasia in MAT-TG (Supplementary Material, Fig. S2).

Methylation status of the BAC-clone allele

Next, to examine the DNA methylation status of imprint-regulatory CpG islands of the BAC-clone derived from the C3H strain mouse genome, we performed bisulphite sequencing (Fig. 3A and B). The mutant allele was distinguished from the genomic allele (B6) by single nucleotide polymorphisms (SNPs) specific to the C3H strain mouse genome: rs47249656 C > T mutation at IG-DMR and rs239260883 G > T mutation at *Gtl2*-DMR. The IG-DMR and *Gtl2*-DMR in the BAC-clone allele were hypermethylated, 94.5 and 98.7%, respectively, in the PAT-TG at embryonic day (E) 9.5. In contrast, these DMRs were hypomethylated, 6.1 and 7.0%, in MAT-TG. The hypermethylation status in PAT-TG and hypomethylation status in the MAT-TG at IG-DMR were maintained at E15.5 in the brain (98.6 vs. 25.7%), lung (96.6 vs. 19.5%), and heart (92.5 vs. 17.4%). The DNA methylation levels of endogenous IG-DMR and *Gtl2*-DMR, which were detected as mean levels of paternal (hypermethylated) and maternal (hypomethylated) alleles, were at the theoretical level of almost 50%. These results revealed that the DMRs of the BAC-clone in the mutants were imprinted as well as those of the endogenous alleles. Therefore, we conclude that the imprinted genes from the BAC-clone allele were being expressed in a parental-origin-dependent manner and that this affected the developmental phenotypes of the mutants.

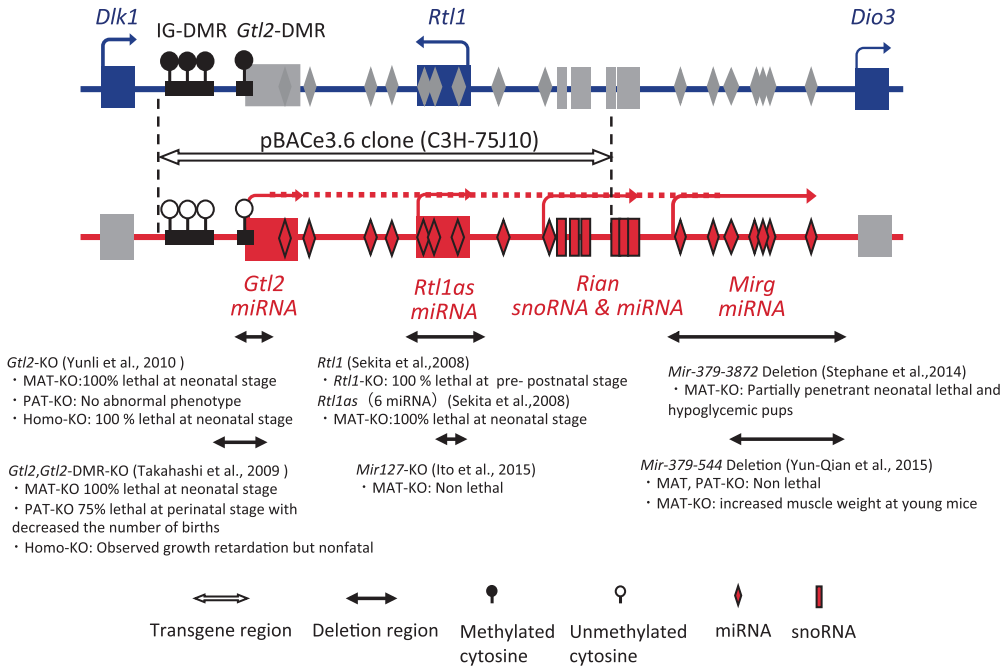

Figure 1. *Dlk1-Dio3* paternally imprinted locus on mouse chromosome 12. From the 1-Mb imprinted locus, the lncRNA genes, *Gtl2*, *Rtl1as*, and *Mirg*, miRNAs, as well as snoRNAs are expressed from the maternally inherited chromosome, whereas the protein-coding genes *Dlk1*, *Dio3*, and *Rtl1* are expressed from the paternally inherited chromosome. Expression of these imprinted genes is regulated by the intergenic-differentially methylated region (IG-DMR) and *Gtl2*-DMR, which are methylated by paternal transmission. Grey boxes represent genes that are repressed. The white left-right arrow indicates the BAC-clone (pBACe3.6) used in this study.

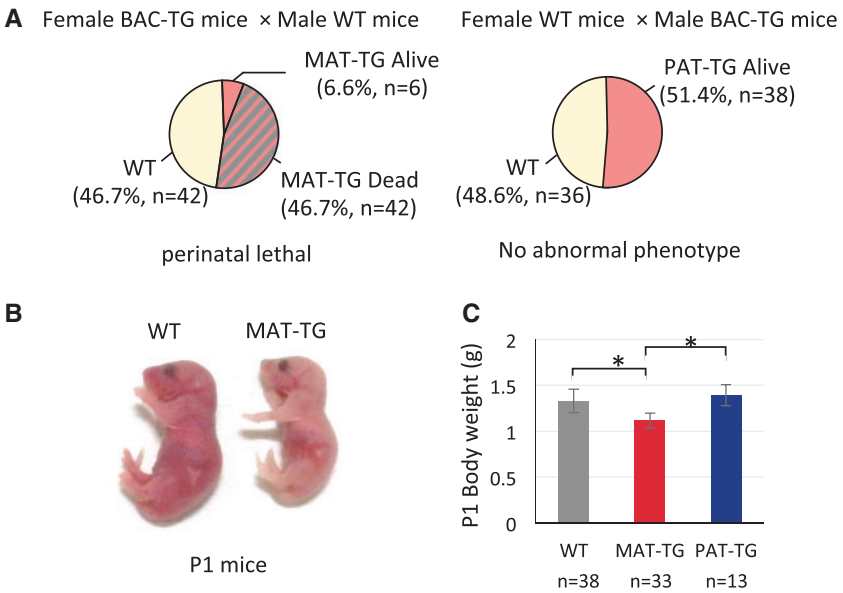

Figure 2. Breeding test of BAC-TG mice and phenotypes of the mutant pups. (**A**) Postnatal lethality of BAC-TG mice. Male and female BAC-TG founder mice were mated with WT of BDF1 mice, and data were obtained from mice of the F3-F5 generations. A total of 88% MAT-TG mice ($n = 42$) experienced postnatal death within 1 week, although this was not observed in PAT-TG mice. (**B**) MAT-TG pups were apparently smaller than PAT-TG and WT pups. (**C**) Birth-body weight of MAT-TG ($n = 38$), PAT-TG ($n = 13$), and WT ($n = 38$) pups. *Significant different by Student's *t*-test at $P < 0.01$.

Gene expression profiling

To gain the further insight into the parental origin-dependent developmental phenotypes of the mutants, we performed of mRNA-Seq and miRNA-Seq analyses by using a next-generation sequencer.

mRNA transcriptome. The transcriptome data of E11.5 mutant foetuses (MAT-TG: $n = 5$, PAT-TG: $n = 4$) were obtained and our RNA-Seq analysis yielded 16.3–21.1 million unique aligned reads (Supplementary Material, Table S1). Assignment to the mouse GRCm38/mm10 reference genome showed that nearly 83–87% of the transcripts encoded proteins, with noncoding genes each accounting for 10–13% of the genes in all profiles (Fig. 4A). The correlation coefficients among the data sets were very high, 0.95–0.97 (Supplementary Material, Fig. S3) with an average number of transcripts of 10,571–10,740.

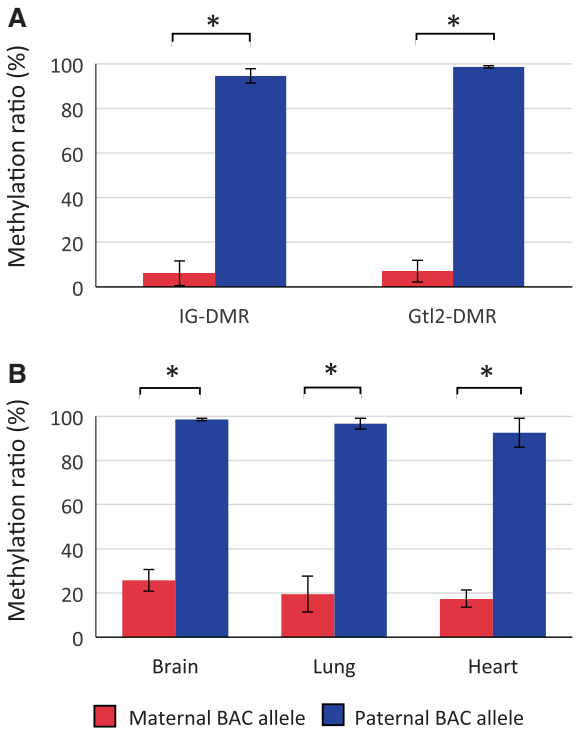

Figure 3. DNA methylation status of IG-DMR and *Gtl2*-DMR in BAC-TG. Methylation levels of IG-DMR (18 CpG sites) and *Gtl2*-DMR (22 CpG sites) of the BAC-encoded allele and WT allele in MAT-TG and PAT-TG foetuses. (**A**) E9.5 whole foetuses ($n = 3$), and (**B**) E15.5 foetal major organs ($n = 3$). The values represent the means ± SD. *Significantly different by Student's *t*-test at $P < 0.01$.

We also analysed genes whose expression was found to be significantly changed in the mutants according to a statistical significance as determined using a moderated *t*-test with a Benjamini-Hochberg false-discovery rate of <0.05. Notably, an overwhelmingly large number of genes showed downregulation, especially in the MAT-TG, wherein 1,500 and 2,131 were upregulated and downregulated, respectively; in the PAT-TG the numbers were 900 and 1,517 (Fig. 4B). Of these, 804 and 869 genes were specifically downregulated and upregulated, respectively (Fig. 4C), demonstrating that a considerable number of genes were commonly changed in MAT-TG and PAT-TG. The top 20 genes upregulated and downregulated in MAT-TG are shown in Figure 4D. Among the downregulated genes, suppressor of cytokine signalling 1 (*Socs1*) (20) and nuclear factor I/X (*Nfix*) (21) have been reported to be associated with perinatal lethality.

To gain insight into the biological functions of the screened genes, we performed GeneOntology (GO) analysis and pathway analysis using genes specifically changed in the MAT-TG and found that the GO terms related to 'cell cycle/division' and 'transcription' were highly enriched (Supplementary Material, Table S2). Furthermore, pathway analysis using the Kyoto Encyclopedia of Genes and Genomes (KEGG) suggested that the genes changed in the MAT-TG were involved in the following pathways: 'Tight junction', 'Pathways in cancer', 'Focal adhesion', 'Nucleotide excision repair', 'RNA degradation', 'DNA replication', and 'Pyruvate metabolism' (Supplementary Material, Table S2).

Genes of the *Dlk1-Dio3* imprinted cluster were expressed in a parental-origin-dependent manner (Fig. 5A). In the MAT-TG, *Gtl2*, *Rtl1/Rtl1as* and *Rian*, were expressed at significantly higher levels than in WT. This tendency was observed in the PAT-TG but the changes were limited, suggesting a leak of these genes from paternally transmitted BAC alleles. Notably, the expression of *Dlk1* and *Mirg*, which were not included in the BAC-clone, was significantly lower in the MAT-TG and PAT-TG mutants than in WT. In the case of *Rlt1* and *Rtl1as*, the expression of these genes could not be detected separately because they are expressed in the reverse direction from the same domain. Thus, we used specific primers and performed quantitative real-time reverse transcription polymerase chain reaction (RT-qPCR) to separately detect the expression levels of *Rtl1* and *Rtl1as*, in which mir127 expression was regarded as *Rtl1as* expression (22) (Fig. 5B). In the MAT-TG *Rtl1* and *Rtl1as* expression showed a drastic inverse correlation, with the levels being 0.4 and 6.0 times than in controls, respectively. In contrast, in the PAT-TG mutants, both genes showed 3-fold higher expression than in controls. This finding indicates that *Rtl1as* expression was related to the methylation imprint status of the BAC-clone allele.

Furthermore, among the downregulated genes in the MAT-TG, 24 represented the targets of miRNAs generated from the BAC-clone locus (Fig. 4D). The relevance of this observation will be further supported by miRNA transcriptome results described in the next section.

miRNA transcriptome. The miRNA transcriptome data of E11.5 mutant foetuses (MAT-TG: $n = 3$, PAT-TG: $n = 3$) were obtained. Our miRNA-Seq analysis yielded 4.3–6.8 million unique aligned reads (Supplementary Material, Table S3). The results of the mRNA-Seq transcriptome analysis demonstrated that expression of the 3 noncoding genes in the BAC-clone, *Gtl2, Rtl1as*, and *Rian*, was markedly altered (Fig. 5). This suggested that the expression of miRNAs from the 3 noncoding imprinted transcripts would also be substantially changed and that this would affect the MAT-TG phenotype through mRNA degradation and the translational repression of the target mRNAs. Therefore, we performed miRNA-Seq analysis to elucidate the molecular mechanism underlying the mutant phenotypes.

Of the 1,638 miRNAs identified in mice to date (database miRBase21), 451 miRNAs were detected in any samples and 440, 431, and 412 were detected in the MAT-TG, PAT-TG, and WT, respectively. The miRNAs that were expressed in each group are shown in Figure 6A and Supplementary Material, Table S5. The top 20 miRNAs of each group accounted for >60% of the total reads, and the 3 miRNAs showing highest expression levels, mir10b, mir10a and mir92-1, were common to all three groups and accounted for almost 30% of the total miRNA reads. Here, we focused on the 19 miRNAs, of which 5, 5, and 2 miRNAs, derived from *Gtl2, Rtl1as*, and *Rian*, respectively, were expressed at significantly higher levels in the MAT-TG than in PAT-TG and WT (Fig. 6B), while the expression of 7 other miRNAs was not detected. We speculated that the increased expression of the miRNAs in the MAT-TG, which would be caused by their expression from the BAC-clone allele, might be involved in the observed postnatal lethality. Thus, we checked for the target mRNAs of the miRNAs by using miRDB, which suggested 507 genes as the targets (Supplementary Material, Table S5). Furthermore, to identify genes that were downregulated by the overexpressed miRNAs from the BAC-clone in the MAT-TG, we performed a comparative analysis with the mRNA-Seq datasets. The results identified 24 genes with expression that was specifically decreased in the MAT-TG, as the targets of the miRNAs expressed from the BAC-clone (Fig. 6C). Thus, we obtained information on the mice in which these

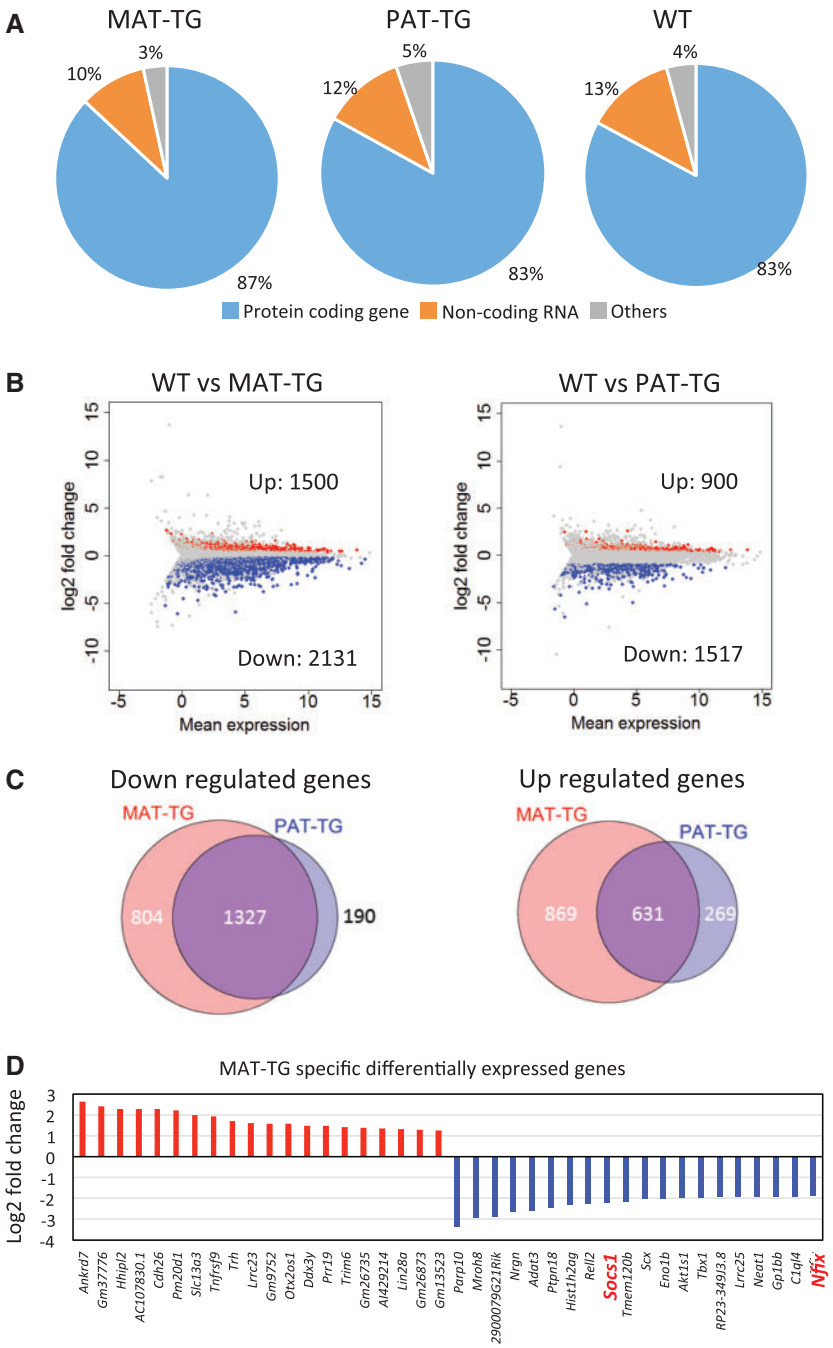

Figure 4. Gene expression profiling of BAC-TG by using mRNA-Seq. (**A**) Pie charts show the composition of reference gene types in the ensemble transcripts data for each RNA-seq data set. (**B**) MA plots show changes in expression levels in MAT-TG and PAT-TG fotuses. The X-axis and Y-axis show the log2 geometric average of gene expression level and the log2 fold change between samples, respectively. Red and blue dots show significantly upregulated and downregulated genes, respectively. (**C**) Pie charts show genes specifically upregulated (left) and downregulated (right) in MAT-TG and PAT-TG. (**D**) Top 20 of up- and downregulated genes in MAT-TG and PAT-TG foetuses.

genes had been knocked out. We found that 9 of the 24 genes had been shown to be involved in specific abnormalities (Fig. 6C) and that the knockout of 3 genes, *Col5a1*, *Pcgf2* and *Clip2*, the targets of mir770, mir493, and mir665, respectively, was reported to result in prenatal and postnatal growth retardation and/or lethality similar to that observed in the MAT-TG in the current study. Therefore, these genes, acting alone or synergistically, might be responsible for the unique phenotype of the MAT-TG mice.

Gene network analysis

To understand the possibility that the repression effect of miRNAs on particular genes (Fig. 4C, $n = 804$) affects further biological defects in the MAT-TG, we performed a network analysis using the Ingenuity Pathway Analysis (IPA) tool. Consequently, a large gene network, which consists of important biological functions, was constructed (Supplementary Material, Fig. S4). This suggests that dysfunction of the network leads to severe defects including lethality at high significance scores

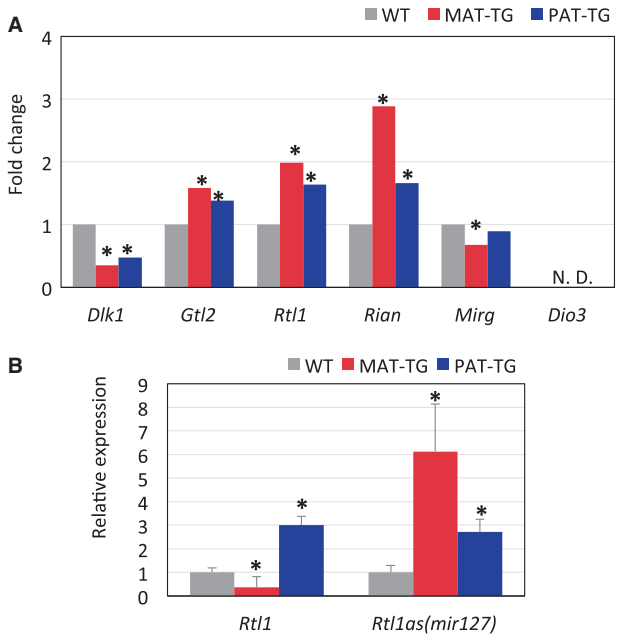

Figure 5. Relative expression levels of the imprinted genes located at the *Dlk1–Dio3* domain in BAC-TG. (**A**) Expression levels of *Dlk1*, *Gtl2*, *Rtl1*, *Mirg*, and *Dio3* in the E9.5 MAT-TG ($n=5$) and PAT-TG ($n=4$) embryos obtained from our transcriptome data. *Significantly differences at $q<0.05$ compared with WT ($n=5$) by FDR. N.D.: not detected. (**B**) Expression levels of *Rtl1* and *Rtl1as* in E15.5 MAT-TG ($n=4$) and PAT-TG ($n=4$) embryos determined by using quantitative RT-PCR. Significantly different at $^*P<0.01$ by Student's *t*-test. The expression level of mi127RNA was shown as that of *Rtl1as*. The expression of *Rtl1* and *Rtl1as* was calibrated by those of *Gapdh* and snoRNA202, respectively. The values represent the means ± SD.

(Supplementary Material, Table S7). Notably, 10 of 24 downregulated target genes, which were targets of miRNA generated from *Gtl2* are included in the network. Of these, *Col5a1, Pcgf2*, and *Clip2* have been reported to cause lethality in null mutants.

Discussion

The *Dlk1-Dio3* imprinted locus is recognised as playing a critical role in embryonic and postnatal development. Maternal and paternal uniparental disomy, epimutation and deletion in this region causes Temple syndrome or Kagami-Ogata syndrome in humans (13,23) and in mice (24). Of particular interest is the function of the miRNA cluster at this locus that is expressed by the maternal allele. A wide range of effects including characteristic functions of miRNAs have been identified by performing *in silico* analyses, some of which have been demonstrated *in vivo* and *in vitro* (25–29). Therefore, we supposed that noncoding RNAs expressed from the imprinting locus, especially miRNAs, could represent the primary cause of the BAC-TG phenotypes observed in this study. To verify our hypothesis, we first examined whether the IG-DMR and *Gtl2*-DMR of the BAC-clone allele was imprinted in the BAC-TG mice. Bisulphite sequence analysis of the IG-DMR and *Gtl2*-DMR demonstrated that the 147-kb BAC clone that contained IG-DMR, *Gtl2*, *Rtl1* and the first half part of *Rian*, fully functioned as a unit of genomic domain for acquiring a paternal methylation imprint. This indicated that the noncoding RNAs were expressed from the BAC derived sequence when the inserted allele was transmitted maternally. From these observations it is suggested that overexpression of noncoding RNAs in the MAT-TG mice may be involved in the parental-origin-dependent postnatal lethality, as the majority of the MAT-TG mice had died within 1 week. A critical aim of this study was to ascertain whether overexpression of miRNAs from the *Gtl2-Rian* domain led to the severe developmental failure in the MAT-TG mice. Therefore, we conducted transcriptome analyses for mRNAs and miRNAs, and then performed *in silico* analysis to identify potential causative miRNAs and their target genes.

Our results demonstrated that the miRNAs markedly induced downregulation of the target genes, and further suggested that the altered expression of the target genes would cause postnatal lethality in the MAT-TG. Focusing on the BAC clone allele, it was found that of 19 miRNA-Sequences encoded by the BAC allele, 12 were expressed in the MAT-TG foetuses at 2–5-fold higher levels than in controls. However, because the causative candidate miRNAs remained elusive, it was necessary to further narrow the possibilities. The miRNAs expressed from *Rtl1as* are likely to perform important functions. The miRNAs processed from *Rtl1as* degrade *Rtl1* via RNAi mechanism and therefore deletion of *Rtl1as* and mir127 resulted in *Rtl1* overexpression (22). In contrast, overexpression of these miRNAs enhanced degradation of *Rtl1*, and indeed *Rtl1* expression was significantly decreased in the MAT-TG mutants. We cannot rule out the possibility that the decreased *Rtl1* expression affects developmental defects in the MAT-TG mutants. However, MAT-TG was apparently in discord with *Rtl1*-KO embryos. The *Rtl1*-KO embryos exhibited late-fetal or neonatal lethality due to severe defects of placentation (15,30). On the other hand, MAT-TG pups were born at the theoretical ratio and died within a week after birth. From the clear differences between them, we hypothesized that miRNAs generated from the BAC locus, rather than the decreased expression of *Rtl1*, were more likely the cause of the MAT-TG lethality. Another paternally expressed gene *Dlk1* was decreased in both the MAT-TG and PAT-TG. It might be caused by overexpression of mir127, which targets *Dlk1* and was upregulated in the both mutants. Apparently, the decreased *Dlk1* expression is not a cause of the phenotype of the MAT-TG because the PAT-TG mutants are viable. *Mirg* expression was slightly reduced in the MAT-TG mutants, suggesting that the endogenous noncoding RNAs in the domain was repressed to minimize excess expression of the noncoding RNAs from the BAC.

Currently, no direct evidence is available to indicate that miRNAs expressed from *Gtl2* are involved in the postnatal death. However, several lines of evidence support the hypothesis that miRNAs expressed from *Gtl2* are involved in this phenotype. First, our previous study demonstrated that when the *Gtl2* deletion was maternally inherited, the hetero-mutants exhibited postnatal lethality, whereas the *Gtl2* homo-mutants were normal and survived similar to WT (18). These findings indicate that whereas the deleted *Gtl2* region itself is not the cause of the postnatal death, the miRNAs transcribed from the downstream of *Gtl2* may represent the potential cause. In this case, the depletion of these miRNAs could lead to postnatal death. Furthermore, the *in silico* analysis in the current study yielded the key result that postnatal lethality and embryonic growth retardation could involve genes targeted by those miRNAs expressed from *Gtl2* whose levels were elevated 3.5–4.5-fold relative to controls. As the most influential miRNAs, we identified mir770, mir665, and mir493, because deletion of their target genes, *Col5a1, Clip2, and Pcgf2* has been demonstrated previously to result in severe defects, such as growth retardation and postnatal lethality (31–33). However, the phenotype of the MAT-TG does not necessarily coincide perfectly with these findings.

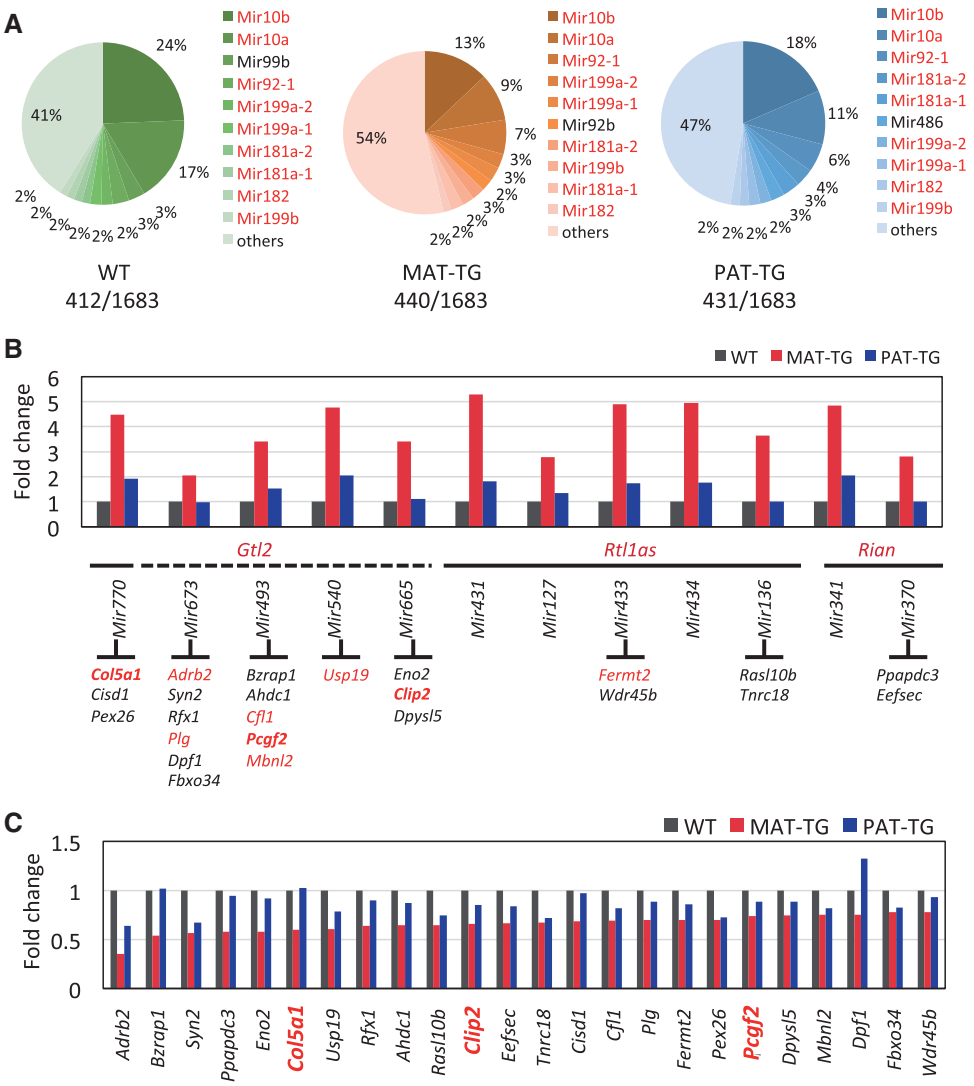

Figure 6. Profiling of miRNA expressions in BAC-TG mouse embryos. (**A**) Pie charts represent the proportions of miRNA expression in E11.5 embryos of MAT-TG, PAT-TG and WT. Of the top 10 miRNAs, the 9 indicated in red text were commonly expressed in MAT-TG, PAT-TG and WT. (**B**) Expression levels of 5, 5, and 2 miRNAs generated from *Gtl2*, *Rtl1as*, and *Rian*, respectively. The 24 target genes that exhibited decreased expression in the MAT-TG embryos are shown under each respective miRNA. Knockout studies have been reported for the 9 target genes indicated in red letters. (**C**) Expression levels of the 24 target genes in MAT-TG, PAT-TG and WT embryos.

Thus, further study is required to understand the mechanism of the lethality.

Gene network analysis provided further evidence that supports our idea that the miRNAs from *Gtl2* are responsible for the MAT-TG lethality. Consequently, the large gene network, which was constructed by downregulated genes in the MAT-TG suggests that dysfunction of the network is involved in the lethality. Notably, 9 of 24 down regulated target genes were targets of miRNAs generated from *Gtl2* and *Rtl1*, and included in the network. Therefore, these genes, functioning alone or synergistically, might be responsible for the unique lethality of the MAT-TG (Fig. 6), although this intriguing possibility remains to be verified experimentally.

The results of the present study also suggest that miRNAs expressed from the *Gtl2* domain in humans are involved in specific diseases. Of the 19 miRNAs that were expressed from the BAC-TG allele in mutant mice, 10 are encoded within the human *Gtl2* domain. These 10 miRNAs target 427 genes of which 128 (9 common with mouse) are involved in 67 human diseases (Supplementary Material, Table. S6). For example, mutation of CNTN1 and SCNN1B, which are targets of mir493 and mir665 generated from GTL2, leads to a phenotype similar to Temple syndrome (34,35). Temple syndrome itself is caused by a disorder of imprinting with the patients exhibiting low birth weight, hypotonia, and short stature. However, to date, no direct evidence has been obtained indicating that the miRNAs expressed from this imprinted locus play a role in specific diseases by regulating the expression of their target genes, a crucial and highly intriguing matter for which clarification is awaited. Overall, the issues shown by the gene network analysis in this study may constitute a representative case, whereby downregulation of gene expressions via the enhanced expression of miRNAs causes a pivotal effect beyond that expected.

Materials and Methods

Ethics statement

All animal procedures were in accordance with the guidelines of the Science Council of Japan, and the experiments were approved by the Institutional Animal Care and Use Committee of the Tokyo University of Agriculture.

Generation of BAC-TG mice

BAC-TG mice harbouring a 147-kb BAC (Vector pBACe3.6; 11490 bp, C3H genomic library), carrying IG-DMR, *Gtl2*, *Rtl1*, and the first half part of *Rian*, were generated through microinjection into the pronucleus of B6D2F1 mice. The vector used was linearised by digesting with *Not I* (Takara Bio, Tokyo, Japan). The MAT-TG and PAT-TG mice were generated through reciprocal mating between the WT (BDF1) and male and female heterozygous BAC-TG mice. The heterozygous BAC-TG line could be maintained only when the transgene was of paternal origin because most of the MAT-TG mice were not viable.

The mutants were genotyped by PCR-amplification with primers specific for the T7 sequence: 5'-TAATACGACTCACTAT AGGG-3' and 5'-CCTGGAGCCTAGCACATTCT-3'. The BAC-TG mice in this study were used for analysis after three generations.

Southern blotting

The copy number of the inserted BAC clone in the BAC-TG mice was determined by performing Southern blotting. Genomic DNA, which was prepared from the lung, was treated with *EcoRV* (New England Biolabs Japan, Tokyo, Japan). The DNA was electrophoresed on 0.7% agarose gels and transferred onto GeneScreen Plus Hybridization Transfer Membranes (PerkinElmer, Waltham, MA, USA), and then blotted and detected using DIG-labelled DNA probes synthesised by using a DIG PCR Synthesis Kit (Roche Diagnostics Japan, Tokyo, Japan) in accordance with the manufacturer's protocol.

Fluorescence *in situ* hybridisation (FISH) mapping analysis

Chromosome preparations were obtained from splenic lymphocytes of the BAC-TG mice as described previously (36,37). The cultured cells were treated with BrdU during late S phase for differential replication banding. R-banded chromosomes were obtained by exposing the chromosome slide to UV light after staining with Hoechst 33258 (Sigma, St. Louis, MO, USA). FISH mapping was performed as described previously (37). The BAC clone was labelled by using a nick-translation kit (Roche) with digoxigenin-11-dUTP (Roche) using a nick-translation kit (Roche), and the fluorescence signal was detected with rhodamine-conjugated anti-digoxigenin Fab fragments (Roche). FISH images were computed with a cooled CCD camera (Leica DFC360 FX, Leica Microsystems, Wetzlar, Germany) mounted on a Leica DMRA microscope and processed using the 550CW-QFISH application program (Leica Microsystem Imaging Solutions, Cambridge, UK).

DNA isolation and methylation analysis

Genomic DNA was isolated from whole embryos at E9.5 and from the heart, lungs, and brain at E15.5 of MAT-TG and PAT-TG mice by using the proteinase K/SDS and phenol-chloroform methods. The DNA (1 μg) was treated with sodium bisulphite by using the an EpiTect Bisulfite Kit (QIAGEN, Venlo, The Netherlands) as described previously (38). The following sequencing primers were used for detecting the methylation status of 18 and 22 CpG sites within IG-DMR and Gtl2-DMR, respectively: IG-DMR: 5'-AGGGTATTATAGAGTAGGTTT-3' and 5'-CTACAATATAAATCAAATACCTTCAAC-3', and *Gtl2*-DMR: 5'-TATAAAATGGGGGGGGGGTATTTG-3' and 5'-CTAACCCACCCCC CACATCT-3'.

To purify the PCR products, the DNA fragments were separated electrophoretically on 2% agarose gels, and the bands were excised and purified using a Wizard SV gel and PCR Clean-Up System (Promega, Madison, WL, USA). Purified DNA was cloned into the pGEM T-Easy Vector (Promega) and sequenced using an ABI PRISM 3130 Genetic Analyzer (Applied Biosystems Japan, Tokyo, Japan). Bisulphite-modification efficiency calculated as the fraction of modified cytosines in non-CpG sequences was exceeded 98%. Each experiment was performed using 3 biological replications. Data quality was evaluated using a quantification tool for methylation analysis and the data that showed >98% conversion rate of CT at CpH were used for further analysis. Homologous sequences were eliminated.

Quantitative real-time reverse transcription (RT)-PCR

Total RNA was isolated from E15.5 whole embryos and from placenta by using TRIzol reagent (Invitrogen, Carlsbad, CA, USA) with DNase (Promega) treatment, and the RNA was reverse-transcribed by using SuperScript III (Life Technologies, Carlsbad, CA, USA) with random hexamers. Real-time PCR was performed using Lightcycler 480 SYBR Green I Master Mix (Roche) on a 7500 Fast Real-Time PCR System (Applied Biosystems). The relative expression level of each gene was normalised to Gapdh expression level and was analysed by means of relative quantification using the ΔΔCt method.

Rtl1as expression

Rtl1as expression was detected as expression of mir127 by using TaqMan MicroRNA Assays (Applied Biosystems). The amount of miRNA in each sample was calibrated against the snoRNA202 expression level. This value was then used to calculate the D threshold cycle (CT) value for each miRNA (miRNA CT value – MBII-143 CT value). Fold-changes were calculated as follows: a unit increase in the CT value was equivalent to a 2-fold increase in expression (ΔΔCT method).

mRNA-seq

Total RNA was isolated from E11.5 whole embryos by using TRIzol reagent with DNase treatment; 5 biological replicates were prepared for each sample. Total RNA (10 ng) samples were used for synthesising cDNA by using the SMARTer Ultra Low Input RNA for Illumina Sequencing -HV and Advantage 2 PCR Kit (Clontech, Mountain View, CA, USA) according to the manufacturer's instructions. Pre-amplified cDNA was fragmented into 200-bp fragments by using an S2 sonicator (Covaris, Woburn, MA, USA) and then used to construct sequencing libraries by using an NEBNext Ultra DNA Library Prep Kit (New England BioLabs, Ipswich, MA, USA). Indexed libraries were pooled (10 nM each), and sequenced using an Illumina HiSeq 2500 (single-end, 51-bp condition) (San Diego, CA, USA).

miRNA-seq data analysis and target-gene prediction

The sequencing libraries for miRNA-Seq were prepared using the TruSeq Small RNA Sample Preparation Kit (Illumina) according to manufacturer's instructions. Total RNA (1 μg) was ligated sequentially to 3' and 5' adaptors. Subsequently, the ligation product was reverse-transcribed and then PCR-amplified for 11 cycles to enrich the miRNAs harbouring adapter sequences on both ends. The amplified cDNA constructs were size-fractionated (145–160 bp) and purified using 6% Novex TBE PAGE gels (Invitrogen). The miRNA library was quantified using qPCR and the size distribution was validated on a 2100 Bioanalyzer (Agilent, Santa Clara, CA, USA) by a high-sensitivity DNA chip. All libraries were sequenced using an Illumina NextSeq 500 (single-end, 51-bp condition).

mRNA-seq and miRNA-seq alignments and statistical analysis

Quality control of mRNA-Seq and miRNA-Seq raw sequencing reads was performed using the Cutadapt v1.11 and Fastq quality trimmers v0.0.13. Trimmed mRNA-Seq reads for each sample were aligned to the mouse genome (mm10, Genome Reference Consortium Mouse Build 38) using the Tophat v2.0.4 (39). Aligned reads were subsequently assembled into transcripts guided by reference annotation (Ensemble gene set). Transcript expression was quantified in terms of reads per million mapped reads and normalised using the RPKM method with Cufflinks v2.0.1.

To identify significant differentially expressed genes between MAT-TG vs wild-type (WT), and PAT-TG vs WT, we used a Cufdiff v2.0.1 with Benjamini-Hochberg false-discovery rate of <0.05. Differentially expressed genes in MAT-TG were used for gene ontology (GO) analysis with the KEGG pathway (Release 81.0) in the DAVID web tool (http://david.abcc.ncifcrf.gov/) (40); a background of all mouse genes was applied. Biological-process term groups with a significance of $P < 0.01$ (Fisher's exact test) were considered significant. The trimmed miRNA-Seq reads were mapped with Bowtie v0.12.8 against mouse genome mm10/GRCm38. Expression intensity was estimated using SeqMonk v0.330 as Read Per Million reads (RPM). We identified miRNA target genes using the miRNA database (miRDB), in which a miRDB target score ≧ 90 was used.

Gene ontology gene-to-gene network analysis using Ingenuity Pathway Analysis (IPA) was also performed. IPA (ver. December 2016, www.ingenuity.com) was performed on MAT-TG specific differentially expressed mRNAs. Each gene identifier was mapped to its corresponding gene object in the Ingenuity Pathways Knowledge Base.

Data Availability

The mRNA-Seq and miRNA-Seq data from this study have been deposited in the DDBJ under the accession number DRA (DRA005596) in the registration process.

Supplementary Material

Supplementary Material is available at *HMG* online.

Acknowledgements

We thank Wu Qiong, Hidehiko Ogawa and Yayoi Obata for helpful comments.

Conflict of Interest statement. None declared.

Funding

Grants-in-Aid for Scientific Research from the Japanese Science and Technology Agency (15H02472) and the Japanese Agency for Medical Research and Development (15gm0510017h0103). Funding to pay the Open Access publication charges for the article was provided by the Japanese Science and Technology Agency.

References

1. Kono, T., Obata, Y., Wu, Q., Niwa, K., Ono, Y., Yamamoto, Y., Park, E.S., Seo, J.S. and Ogawa, H. (2004) Birth of parthenogenetic mice that can develop to adulthood. *Nature*, **428**, 860–864.
2. Kawahara, M., Wu, Q., Yaguchi, Y., Ferguson-Smith, A.C. and Kono, T. (2006) Complementary roles of genes regulated by two paternally methylated imprinted regions on chromosomes 7 and 12 in mouse placentation. *Hum. Mol. Genet.*, **15**, 2869–2879.
3. Kawahara, M., Wu, Q., Takahashi, N., Morita, S., Yamada, K., Ito, M., Ferguson-Smith, A.C. and Kono, T. (2007) High-frequency generation of viable mice from engineered bimaternal embryos. *Nat. Biotechnol.*, **25**, 1045–1050.
4. Ferguson-Smith, A.C. (2011) Genomic imprinting: the emergence of an epigenetic paradigm. *Nat. Rev. Genet.*, **12**, 565–575.
5. Miyoshi, N., Wagatsuma, H., Wakana, S., Shiroishi, T., Nomura, M., Aisaka, K., Kohda, T., Surani, M.A., Kaneko-Ishino, T. and Ishino, F. (2000) Identification of an imprinted gene, Meg3/Gtl2 and its human homologue MEG3, first mapped on mouse distal chromosome 12 and human chromosome 14q. *Genes Cells*, **5**, 211–220.
6. Schmidt, J.V., Matteson, P.G., Jones, B.K., Guan, X.J. and Tilghman, S.M. (2000) The Dlk1 and Gtl2 genes are linked and reciprocally imprinted. *Genes Dev.*, **14**, 1997–2002.
7. Hatada, I., Morita, S., Obata, Y., Sotomaru, Y., Shimoda, M. and Kono, T. (2001) Identification of a new imprinted gene, Rian, on mouse chromosome 12 by fluorescent differential display screening. *J. Biochem.*, **130**, 187–190.
8. Hernandez, A., Fiering, S., Martinez, E., Galton, V.A. and St Germain, D. (2002) The gene locus encoding iodothyronine deiodinase type 3 (Dio3) is imprinted in the fetus and expresses antisense transcripts. *Endocrinology*, **143**, 4483–4486.
9. Seitz, H., Youngson, N., Lin, S.P., Dalbert, S., Paulsen, M., Bachellerie, J.P., Ferguson-Smith, A.C. and Cavaille, J. (2003) Imprinted microRNA genes transcribed antisense to a reciprocally imprinted retrotransposon-like gene. *Nat. Genet.*, **34**, 261–262.
10. Takada, S., Tevendale, M., Baker, J., Georgiades, P., Campbell, E., Freeman, T., Johnson, M.H., Paulsen, M. and Ferguson-Smith, A.C. (2000) Delta-like and gtl2 are reciprocally expressed, differentially methylated linked imprinted genes on mouse chromosome 12. *Curr. Biol.*, **10**, 1135–1138.
11. Gagne, A., Hochman, A., Qureshi, M., Tong, C., Arbon, J., McDaniel, K. and Davis, T.L. (2014) Analysis of DNA methylation acquisition at the imprinted Dlk1 locus reveals asymmetry at CpG dyads. *Epigenetics Chromatin*, **7**, 9.
12. Ogata, T., Kagami, M. and Ferguson-Smith, A.C. (2008) Molecular mechanisms regulating phenotypic outcome in paternal and maternal uniparental disomy for chromosome 14. *Epigenetics*, **3**, 181–187.

13. Ioannides, Y., Lokulo-Sodipe, K., Mackay, D.J., Davies, J.H. and Temple, I.K. (2014) Temple syndrome: improving the recognition of an underdiagnosed chromosome 14 imprinting disorder: an analysis of 51 published cases. *J. Med. Genet.*, **51**, 495–501.
14. Moon, Y.S., Smas, C.M., Lee, K., Villena, J.A., Kim, K.H., Yun, E.J. and Sul, H.S. (2002) Mice lacking paternally expressed Pref-1/Dlk1 display growth retardation and accelerated adiposity. *Mol. Cell Biol.*, **22**, 5585–5592.
15. Sekita, Y., Wagatsuma, H., Nakamura, K., Ono, R., Kagami, M., Wakisaka, N., Hino, T., Suzuki-Migishima, R., Kohda, T., Ogura, A. *et al.* (2008) Role of retrotransposon-derived imprinted gene, Rtl1, in the feto-maternal interface of mouse placenta. *Nat. Genet.*, **40**, 243–248.
16. Davis, E., Caiment, F., Tordoir, X., Cavaille, J., Ferguson-Smith, A., Cockett, N., Georges, M. and Charlier, C. (2005) RNAi-mediated allelic trans-interaction at the imprinted Rtl1/Peg11 locus. *Curr. Biol.*, **15**, 743–749.
17. Hernandez, A., Martinez, M.E., Fiering, S., Galton, V.A. and St Germain, D. (2006) Type 3 deiodinase is critical for the maturation and function of the thyroid axis. *J. Clin. Invest.*, **116**, 476–484.
18. Takahashi, N., Okamoto, A., Kobayashi, R., Shirai, M., Obata, Y., Ogawa, H., Sotomaru, Y. and Kono, T. (2009) Deletion of Gtl2, imprinted non-coding RNA, with its differentially methylated region induces lethal parent-origin-dependent defects in mice. *Hum. Mol. Genet.*, **18**, 1879–1888.
19. Charalambous, M., Da Rocha, S.T., Radford, E.J., Medina-Gomez, G., Curran, S., Pinnock, S.B., Ferron, S.R., Vidal-Puig, A. and Ferguson-Smith, A.C. (2014) DLK1/PREF1 regulates nutrient metabolism and protects from steatosis. *Proc. Natl. Acad. Sci. U. S. A*, **111**, 16088–16093.
20. Marine, J.C., Topham, D.J., McKay, C., Wang, D., Parganas, E., Stravopodis, D., Yoshimura, A. and Ihle, J.N. (1999) SOCS1 deficiency causes a lymphocyte-dependent perinatal lethality. *Cell*, **98**, 609–616.
21. Driller, K., Pagenstecher, A., Uhl, M., Omran, H., Berlis, A., Grunder, A. and Sippel, A.E. (2007) Nuclear factor I X deficiency causes brain malformation and severe skeletal defects. *Mol. Cell Biol.*, **27**, 3855–3867.
22. Ito, M., Sferruzzi-Perri, A.N., Edwards, C.A., Adalsteinsson, B.T., Allen, S.E., Loo, T.H., Kitazawa, M., Kaneko-Ishino, T., Ishino, F., Stewart, C.L. *et al.* (2015) A trans-homologue interaction between reciprocally imprinted miR-127 and Rtl1 regulates placenta development. *Development*, **142**, 2425–2430.
23. Kagami, M., O'Sullivan, M.J., Green, A.J., Watabe, Y., Arisaka, O., Masawa, N., Matsuoka, K., Fukami, M., Matsubara, K., Kato, F. *et al.* (2010) The IG-DMR and the MEG3-DMR at human chromosome 14q32.2: hierarchical interaction and distinct functional properties as imprinting control centers. *PLoS Genet.*, **6**, e1000992.
24. Georgiades, P., Watkins, M., Surani, M.A. and Ferguson-Smith, A.C. (2000) Parental origin-specific developmental defects in mice with uniparental disomy for chromosome 12. *Development*, **127**, 4719–4728.
25. Takahashi, N., Yamaguchi, E., Kawabata, Y. and Kono, T. (2015) Deleting maternal Gtl2 leads to growth enhancement and decreased expression of stem cell markers in teratoma. *J. Reprod. Dev.*, **61**, 7–12.
26. Valdmanis, P.N., Roy-Chaudhuri, B., Kim, H.K., Sayles, L.C., Zheng, Y., Chuang, C.H., Caswell, D.R., Chu, K., Zhang, Y., Winslow, M.M. *et al.* (2015) Upregulation of the microRNA cluster at the Dlk1-Dio3 locus in lung adenocarcinoma. *Oncogene*, **34**, 94–103.
27. Dai, R., Lu, R. and Ahmed, S.A. (2016) The Upregulation of Genomic Imprinted DLK1-Dio3 miRNAs in Murine Lupus Is Associated with Global DNA Hypomethylation. *PLoS One*, **11**, e0153509.
28. Benetatos, L., Vartholomatos, G. and Hatzimichael, E. (2014) DLK1-DIO3 imprinted cluster in induced pluripotency: landscape in the mist. *Cell Mol. Life Sci.*, **71**, 4421–4430.
29. Mo, C.F., Wu, F.C., Tai, K.Y., Chang, W.C., Chang, K.W., Kuo, H.C., Ho, H.N., Chen, H.F. and Lin, S.P. (2015) Loss of noncoding RNA expression from the DLK1-DIO3 imprinted locus correlates with reduced neural differentiation potential in human embryonic stem cell lines. *Stem Cell Res. Ther.*, **6**, 1.
30. Kitazawa, M., Tamura, M., Kaneko-Ishino, T. and Ishino, F. (2017) Severe damage to the placental fetal capillary network causes mid- to late fetal lethality and reduction in placental size in Peg11/Rtl1 KO mice. *Genes Cells*, **22**, 174–188.
31. Akasaka, T., Kanno, M., Balling, R., Mieza, M.A., Taniguchi, M. and Koseki, H. (1996) A role for mel-18, a Polycomb group-related vertebrate gene, during theanteroposterior specification of the axial skeleton. *Development*, **122**, 1513–1522.
32. Hoogenraad, C.C., Koekkoek, B., Akhmanova, A., Krugers, H., Dortland, B., Miedema, M., van Alphen, A., Kistler, W.M., Jaegle, M., Koutsourakis, M. *et al.* (2002) Targeted mutation of Cyln2 in the Williams syndrome critical region links CLIP-115 haploinsufficiency to neurodevelopmental abnormalities in mice. *Nat. Genet.*, **32**, 116–127.
33. Wenstrup, R.J., Florer, J.B., Brunskill, E.W., Bell, S.M., Chervoneva, I. and Birk, D.E. (2004) Type V collagen controls the initiation of collagen fibril assembly. *J. Biol. Chem.*, **279**, 53331–53337.
34. Compton, A.G., Albrecht, D.E., Seto, J.T., Cooper, S.T., Ilkovski, B., Jones, K.J., Challis, D., Mowat, D., Ranscht, B., Bahlo, M. *et al.* (2008) Mutations in contactin-1, a neural adhesion and neuromuscular junction protein, cause a familial form of lethal congenital myopathy. *Am. J. Hum. Genet.*, **83**, 714–724.
35. Fajac, I., Viel, M., Sublemontier, S., Hubert, D. and Bienvenu, T. (2008) Could a defective epithelial sodium channel lead to bronchiectasis. *Respir. Res.*, **9**, 46.
36. Matsuda, Y., Harada, Y.N., Natsuume-Sakai, S., Lee, K., Shiomi, T. and Chapman, V.M. (1992) Location of the mouse complement factor H gene (cfh) by FISH analysis and replication R-banding. *Cytogenet. Cell Genet.*, **61**, 282–285.
37. Matsuda, Y. and Chapman, V.M. (1995) Application of fluorescence in situ hybridization in genome analysis of the mouse. *Electrophoresis*, **16**, 261–272.
38. Hiura, H., Komiyama, J., Shirai, M., Obata, Y., Ogawa, H. and Kono, T. (2007) DNA methylation imprints on the IG-DMR of the Dlk1-Gtl2 domain in mouse male germline. *FEBS Lett.*, **581**, 1255–1260.
39. Trapnell, C., Roberts, A., Goff, L., Pertea, G., Kim, D., Kelley, D.R., Pimentel, H., Salzberg, S.L., Rinn, J.L. and Pachter, L. (2012) Differential gene and transcript expression analysis of RNA-seq experiments with TopHat and Cufflinks. *Nat. Protoc.*, **7**, 562–578.
40. Huang da, W., Sherman, B.T. and Lempicki, R.A. (2009) Systematic and integrative analysis of large gene lists using DAVID bioinformatics resources. *Nat. Protoc.*, **4**, 44–57.